MADRID
inter.noise 2019
June 16 - 19
NOISE CONTROL FOR A BETTER ENVIRONMENT

Numerical investigation of screech tones in 3-D modes by using an inviscid approach

Lee, Incheol[1]
Beijing Aeronautical Science and Technology Research Institute of COMAC,
Beijing Key Laboratory of Simulation Technology for Civil Aircraft Design
China North of Future Science Park, Changping District Beijing, 102211 P. R. China

Lee, Duck Joo[2]
Korea Advanced Institute of Science and Technology
291 Daehak-Ro, Yuseong-Gu, Daejeon 34141, Republic of Korea

ABSTRACT

Screech tones from supersonic inviscid jet were numerically investigated using computational aeroacoustics methods. A fourth order optimized compact scheme and fourth order Runge-Kutta scheme were used to solve three dimensional Euler equations. The tool was validated at the conditions of two supersonic flows: one is a perfectly expanded jet, and the other is three under-expanded jets. Extensive analysis was performed to investigate the characteristics of two three-dimensional modes, known as B and C modes, of screech tones including two mode transitions for various Mach numbers from 1.2 to 1.9. The directivity of a B-mode screech is investigated with the spectra of a Mach 1.3 jet. The directivity of B-mode screech tones is similar to the directivity of an acoustic dipole, whereas the directivity of C-mode screech tones is close to the directivity of an acoustic monopole. The wavelengths and amplitude of the reproduced screech tones showed good agreement with other results. The azimuthal directivity of both B and C modes becomes asymmetric after the second mode transition. It can be concluded that the present inviscid tool can numerically reproduce the screech tone including its non-linear mode transition without considering a viscous effect.

Keywords: Supersonic jet, Screech tone, Jet noise, Feedback, Shock cell
I-INCE Classification of Subject Number: 76

1. INTRODUCTION

Screech tone has been spotlighted for several decades due to its tonal characteristic and nonlinear modal transitions when jet Mach number varies. Since the first observation by Powell [1] in 1953, there have been a great number of experimental works for the investigation of the characteristics of screech tones; e.g., Davis & Oldfield [2], Rosfjord & Toms [3], Norum [4], Seiner et al. [5], Ponton & Seiner [6], Panda [7] Edgington-Mitchell et al. [8], and Mercier et al. [9], to name just a few. There have been also several approaches using mathematical models to identify the generation mechanism [10,11] and the harmonics of

[1] incheol.lee2@gmail.com
[2] djlee@kaist.ac.kr

screech tones [12], and to predict the frequency and amplitude [13,14].

From the 1990s, various numerical analyses were carried out on the axisymmetric modes, A1 and A2 modes, in 2-D computational domains [15–21]. Since the early 2000s, the numerical work has been expanded to the 3-D computational domain with the help of high-performance computing to investigate the characteristics of two three-dimensional modes, B and C modes. Shen & Tam [22] and Li & Gao [23,24] solved the axisymmetric and three-dimensional unsteady Reynolds average Navier-Stokes (URANS) equations. Kurbatskii [25] used commercial software, ANSYS FLUENT to investigate the characteristics of screech tones. All of them used different k-ε models to consider the effect of turbulence while Gojun and Bogey [26] reproduced the screech tone a compressible large eddy simulation (LES). The majority of the above numerical investigations were done by solving Navier-Stokes equations to consider the viscous effect and small-scale turbulent effect. Only the work performed by Lee & Lee [21] showed an inviscid approach by solving Euler equations; however the approach was limited to the screech tones of axisymmetric modes.

Is it necessary to consider the effect of viscosity and small-scale turbulence when numerically reproducing screech tones of three dimensional as well as axisymmetric modes? Until the 1960s, it was universally accepted that jet turbulence consists of numerous small eddies distributed throughout the jet. [27]. Crow & Champagne [28] and Brown & Roshko [29] were the first to report the observation of large coherent structures in turbulent jets and free shear layers in addition to classical small-scale turbulence. After their research, there has been a variety of approaches focused on the experimental and numerical investigations of turbulent structures of two scales.

It has been confirmed that screech tones are generated by the interaction the shock-cell structure and the vortices induced by downstream-traveling flow instabilities in the core region of the jet. Loh and Hultgren [30] asserted that screech in axisymmetric modes is essentially an inviscid phenomenon. Viswanathan [31] mentioned that no intrinsic timescale exists in the jet core region since the viscosity effect is negligible, and high-Reynolds-number jets are inviscid. Mankbadi et al. [32] numerically solved three dimensional Euler equations to predict the broadband noise propagating to the downstream direction, and their directivity result is comparable to the experimental data. Cheng & Lee [33] conducted numerical simulations of the supersonic jet flow of Mach number of 1.96 by solving two dimensional Euler equations and verified that the near-flow field around the nozzle exit could be numerically simulated without including a turbulence model. Lee & Lee [34] proposed a new prediction formula for the frequency of screech tones in axisymmetric modes based on their numerical simulation of two-dimensional Euler equations.

However, the inviscid approach has not been applied for the analysis of three-dimensional screech of which physics is more complicated than that of axisymmetric screech. In this paper, the three-dimensional Euler equations are solved to investigate the frequency and amplitude characteristics of screech tones in three-dimensional modes without considering the viscous effect. The far-field directivity, as well as the azimuthal directivity as a function of a jet Mach number, are also analyzed.

2. GOVERNING EQUATIONS AND NUMERICAL TECHNIQUES

2.1 Governing equations

In this study, the unsteady, compressible three-dimensional Euler equation was solved as the governing equation. The equation consists of the continuity equation, the

momentum equations in x, y, and z-direction, and the energy equation while no viscous effect is included.

The equation in the conservative form is expressed as:

$$\frac{\partial \boldsymbol{Q}}{\partial t}+\frac{\partial \boldsymbol{E}}{\partial x}+\frac{\partial \boldsymbol{F}}{\partial y}+\frac{\partial \boldsymbol{G}}{\partial z}=0 \tag{1}$$

The dependent variable vector and the inviscid flux vector are expressed as follows:

$$\boldsymbol{Q}=\left[\rho,\rho u,\rho v,\rho w,\rho e_t\right]^T,$$

$$\boldsymbol{E}=\left[\rho u,\rho u^2+p,\rho vu,\rho wu,\left(\rho e_t+p\right)u\right]^T,$$

$$\boldsymbol{F}=\left[\rho v,\rho uv,\rho v^2+p,\rho wv,\left(\rho e_t+p\right)v\right]^T,$$

$$\boldsymbol{G}=\left[\rho w,\rho uw,\rho vw,\rho w^2+p,\left(\rho e_t+p\right)w\right]^T \tag{2}$$

2.1 Numerical methods

Generally, the amplitude of acoustics is less than 4th order of the flow. And there exist many methods [35,36] to analyze noise of small amplitude precisely. In this paper, the fourth-order optimized high order compact (OHOC) scheme [37], is used for the evaluation of spatial derivatives and the fourth-order Runge-Kutta scheme is used for the integration in time. To prevent unwanted non-physical reflections around the computational boundaries, we use generalized characteristic boundary conditions [38] as the time-dependent boundary conditions. Also, artificial dissipation model developed by Kim and Lee [39] and absorbing layer technique is applied. Lee and Lee [40] demonstrated the feasibility of these numerical schemes by performing numerical simulation of jet flow at the initial stage, which shows the generation of axisymmetric screech tones.

Figure 1 shows the schematic sectional view of the computational domain that consists of three sub computational domains. The nozzle exit plane is set to x/D = 0, where D represents the nozzle diameter at the nozzle exit. The computational domain in the axial direction (x) is from 20D to 30D, and that in the radial direction (y) is from the center to 30D. The thickness of the nozzle is set to 0.625D to be comparable to the experiment conducted by Ponton et al. [41] . The absorbing layer, marked as grey in the figure, was attached along the outer boundary of the computational domain to minimize nonphysical reflection at the computational boundaries. The overall number of grid points is about 180,000. The grids were clustered around the nozzle exit, and the smallest size of the grid is 0.02D by 0.02D. The slip wall boundary condition (dotted sections) was applied along the wall edges, and the nonreflecting boundary condition (diagonal stripes) was applied on the boundaries of the far field. The supersonic inflow condition is imposed on the left boundary of the sub-domain 1, and it can be expressed as follows [19] using the ideal gas equation and the isentropic relations:

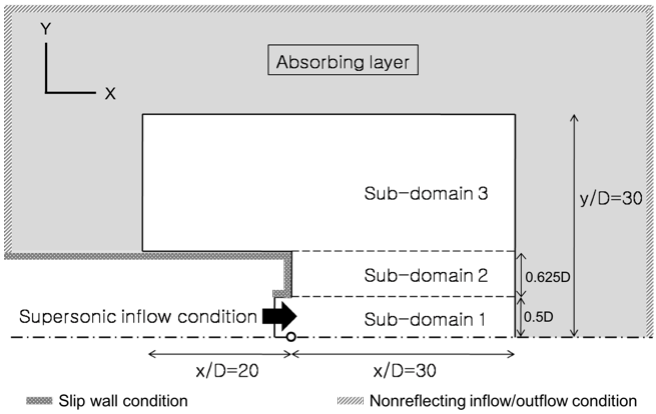

Figure 1 The schematic sectional view of the computational domain

$$\rho_e = \frac{\gamma(\gamma+1)p_e}{2T_r},$$

$$p_e = \frac{1}{\gamma}\left[\frac{2+(\gamma+1)M_j^2}{\gamma+1}\right]^{\frac{\gamma}{\gamma-1}},$$

$$u_e = \left(\frac{2T_r}{\gamma+1}\right)^{\frac{1}{2}}, \qquad v_e = 0 \tag{3}$$

where $T_r = 1$ in this paper to simulate unheated (cold) jet conditions.

Figure 2 shows how the three-dimensional computational domain was composed of the two-dimensional domain introduced in Figure 1. A brief parametric study on the number of sections in the azimuthal direction (φ) were conducted, and it was found that no noticeable difference was observed between $n_\varphi = 36$ and 72. Thus, it was decided to set 36 sectional domains in the azimuthal direction, and the total number of grid points for the computational domain including the absorbing layer is around 6.5 million.

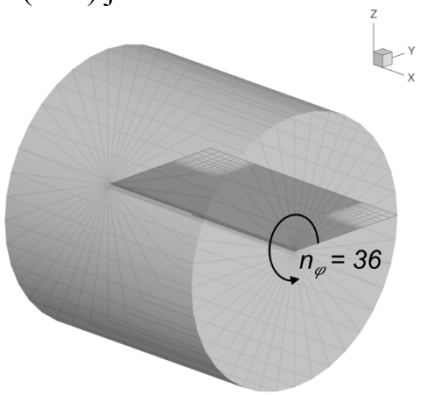

Figure 2 Composition of the three-dimensional computational domain

3. RESULTS AND DISCUSSION

3.1 Validation of flow field

The proposed three-dimensional inviscid approach was validated with two experimental results. A perfectly expanded jet of a Mach number of 2.1 was numerically simulated. Since the jet was perfectly expanded, the inflow condition was not determined by the supersonic inflow condition shown in equation (3). Instead, the inflow pressure and density conditions at the nozzle exit were set to the ambient values whereas the inflow Mach number was set to 2.1. Figure 3 shows the radial Mach-number profiles of the experimental data (symbol) obtained by Troutt & Mclaughlin [42], the present result (thick line) and two axisymmetric numerical results: one was obtained by solving two-dimensional Euler equations (thin line), and the other was obtained by solving two-dimensional Navier-Stokes equations [43] (dash-dot line) at x/D = 1, 5, and 10.

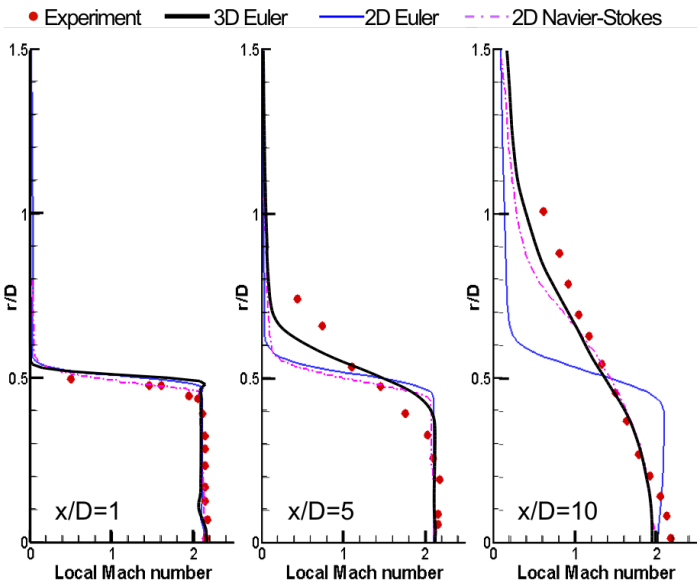

Figure 3 Radial Mach number distributions of perfectly expanded jet of a Mach number of 2.1

Just at the nozzle exit (x/D = 1), all distributions look similar since the jet flow is strong and the initial velocity profile is maintained. As the flow goes downstream, the

experimental results show the three-dimensional diffusion effect and the jet flow spreads in radial direction since supersonic eddies or vortices are generated, and the initial velocity profile is not maintained at downstream. Present three-dimensional results and the two-dimensional results also show a similar trend; however, the results of two-dimensional do not vary significantly for different locations. The initial velocity profile is almost maintained at x/D = 10 even though supersonic eddies or vortices are generated downstream in the two-dimensional Euler simulation. It can be concluded that the effect of three-dimensional diffusion is as much important as the effect of the viscous term in Navier-Stokes equations.

For more quantitative validation, the time average radial density for M_j = 1.43, 1.6, and 1.8 jets at various axial positions downstream from the nozzle exit is calculated and compared with Panda & Seasholtz's experimental results [44] (symbol) and Li & Gao's Navier-Stokes simulation [24] (dashed line) as shown in Figure 4. Note that each plot is shifted by three minor division, and only the experimental data were compared since no other numerical result is available for M_j = 1.80. At the two low jet Mach numbers, very good agreement has been achieved except the region between x/D = 1.2 and 1.55. At M_j = 1.80, more discrepancy between the experimental data and the numerical result is observed, but the overall density distribution of the numerical result seems to be reasonable. The present results show similar results with the other numerical results. It can be concluded that Euler equations may provide similar results with Navier-Stokes equations including turbulence models. Thus, Euler equations may be more effective to simulate screech tones numerically considering computation time and cost.

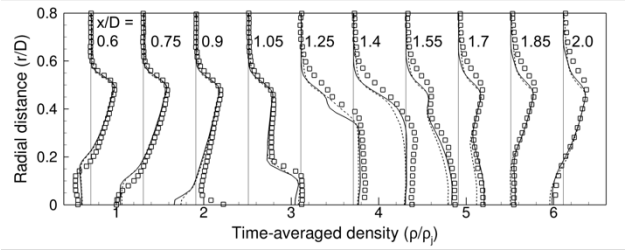

(a) M_j = 1.43

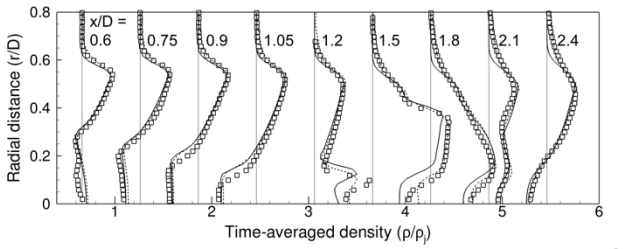

(b) M_j = 1.60

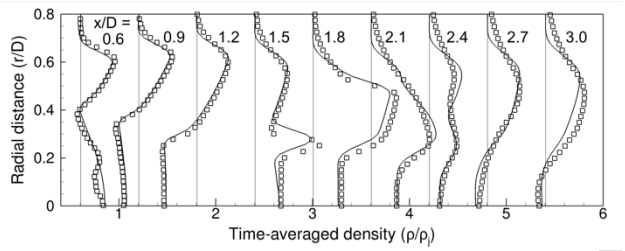

(c) M_j = 1.80

Figure 4 Comparison of time-averaged radial density distribution (symbol: experimental data; solid line: present results; and dashed line: other numerical results)

Through the two validation cases, perfectly expanded and under-expanded jets, the flow field near the nozzle exit calculated by the present three-dimensional inviscid approach is presented. The present method can numerically reproduce the flow structure such as shock cells near the nozzle exit which is critical for the generation of screech tones. Thus, it is expected that the present method can simulate screech tone in three-dimensional modes at various jet Mach numbers.

3.2 Directivity characteristics of screech tones

The spectra of a Mach 1.3 jet at the nozzle exit (x/D = 0, r/D = 0.889) at various azimuthal angles are shown in Figure 5. To make it sure that a screech is fully stabilized, the time signal was obtained after 400,000 iterations. The time signal was recorded for more than 150 dimensionless time that is non-dimensionalized by the nozzle exit diameter and the ambient speed of sound. The recorded time signal is converted to a spectrum in the frequency domain by performing a fast Fourier transform with the application of a Hanning window. The spectra on the plane of the nozzle exit at five azimuthal angles (φ), from 0 to 160 degrees, are presented. In the figure, the x-axis represents a non-dimensionalized frequency and the y-axis represents the SPL (sound pressure level) with a reference of 20 μPa. Note that the spectra of five azimuthal angles have been spaced apart to enhance visual observation. The value of the fundamental tone at each azimuthal angle is shown for reference, and the fundamental tones and the harmonics are marked as dashed lines.

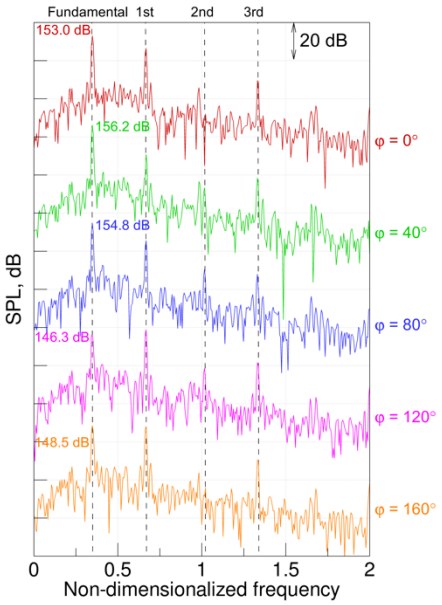

Figure 5 Spectra of a Mach 1.3 jet at various azimuthal angles (x/D = 0, r/D = 0.889)

The fundamental tone and its harmonics are clearly observed at various azimuthal angles. At φ = 0, 40, and 80 degrees, the fundamental tone is greater than the first harmonic and at φ = 120 and 160, the fundamental is smaller than the first harmonic. It is also observed that the amplitude of the fundamental and the second harmonic varies considerably along the azimuthal direction, whereas that of the first and third harmonics are relatively invariant.

To identify the directivity characteristics of a Mach 1.3 jet in the azimuthal direction, the amplitude of the fundamental tone and harmonics is calculated for all grid points on a circle at the nozzle exit (x/D = 0, r/D = 0.889) and shown in Figure 6. The solid line represents the fundamental tone, the dashed line does the first harmonic, the dash-double-dotted line does the second harmonic, and the long-dashed line does the third harmonic, respectively. Since the Mach number 1.30 is supposed to generate a B-mode screech tone, the plane which includes the main directivity is defined as 'BB plane' and shown in the figure. The main directivity of the same jet Mach number investigated by Shen & Tam [22] is shown in the figure as well.

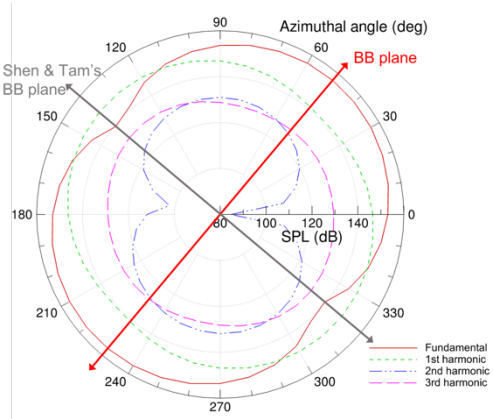

Figure 6 Fundamental tone and its harmonics of a Mach 1.3 jet

It is clearly observed that the directivity pattern resembles that of an acoustic dipole. This is reasonable since a B-mode screech tone has been known to be generated by a flapping motion of the jet flow. However, it is interesting that the direction of the major propagation is different for each tone. For instance, the fundamental tone (solid line) propagates to the direction of φ = 50 and 230 degrees and the second harmonic (dash-double-dotted line) propagates to the direction of φ

= 90 and 270 degrees. This means there would exist an additional factor which alters the directivity of the harmonics. But the factor is not easy to be identified because the maximum amplitude difference between the fundamental tone and the second harmonic is more than 25 dB. The amplitude variation in the azimuthal direction is about 15 dB for the fundamental tone and about 40 dB for the second harmonic. Whereas the amplitude variation is about 10 dB for the first harmonic and less than 5 dB for the third harmonic. This observation is consistent with the observation in Figure 5.

Figure 7 shows the instantaneous non-dimensional density contour of a Mach 1.3 jet on two *r*-*x* planes. To clearly observe the characteristics of noise propagation, the rage of density is limited as $0.995 < \rho/\rho_a < 1.005$. The left-hand side contour shows the noise propagation on BB plane (φ = 50 and 230 degrees) and the right-hand side contour shows the noise propagation on the plane (φ = 140 and 320 degrees) perpendicular to BB plane. On both planes, density fluctuation propagating upstream and downstream is clearly observed. Noise propagation to the upstream direction with a clear regular pattern is the B-mode screech tone. Another component that propagates to the radial direction (± *r*) near the nozzle exit is also clearly observed, which is supposed to be a part of shock associated noise.

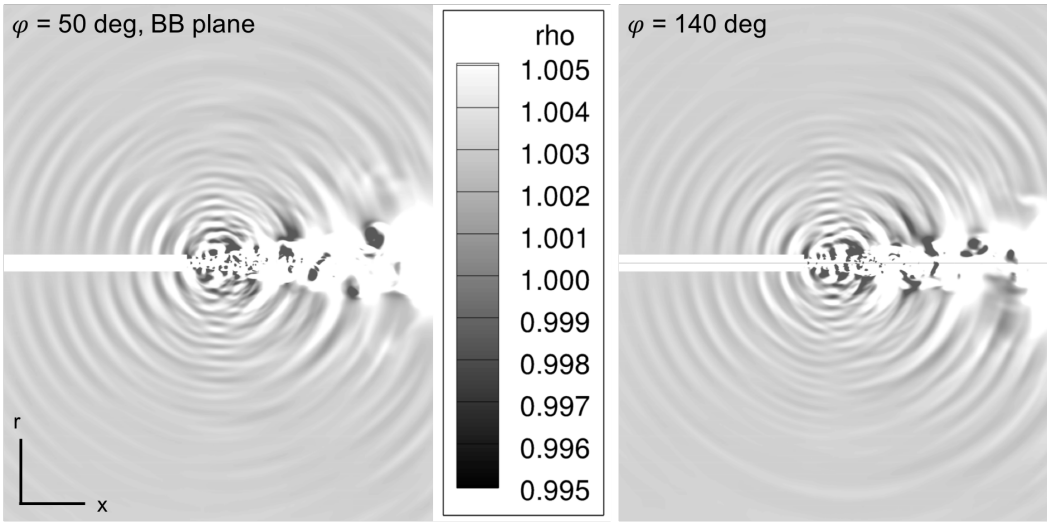

Figure 7 Instantaneous non-dimensional density contour of a Mach 1.3 jet in two planes ($0.995 < \rho/\rho_a < 1.005$, left: BB plane; and right: plane perpendicular to BB plane)

The non-dimensional wavelengths and amplitudes of numerically reproduced screech tones are compared to the experimental data obtained by Ponton et al. [41] and the numerical data carried out by Li & Gao [24] in Figure 8. The time signal was obtained at *r*/D = 2 in the nozzle exit plane for the jet Mach number range from 1.20 to 1.90. As observed in Figure 6, each mode may have its own azimuthal directivity; the maximum amplitude was chosen to represent the amplitude of a specific mode at a jet Mach number. The non-dimensional wavelength of screech tone is defined by the following equation:

$$\frac{\lambda}{D} = \frac{c}{fD} \tag{4}$$

where λ is the wavelength of the screech tone, *c* is the speed of sound, and *f* is the frequency of the tone screech.

In the left-hand side of Figure 8, the calculated wavelengths of three-

dimensional modes show excellent agreement with experimental measurements and other numerical results. In the right-hand side of Figure 8, the calculated SPL values are found to agree favorably with experimental measurements and other numerical results. As introduced in section 1, there are two three-dimensional modes of screech tones, B and C, and both of them are clearly observed with two non-linear mode transitions at certain jet Mach numbers. Ponton et al.'s experimental results show that the first non-linear mode transition from B to C modes occurs at the jet Mach number 1.39. Li & Gao's Navier-Stokes simulations show that the mode transition occurs at the jet Mach number 1.40. The present results show that the mode transition occurs at the jet Mach number 1.36. The experimental data show that the second mode transition from C to B modes occurs at the jet Mach number 1.60 and the present results show that it occurs at the jet Mach number between 1.65 and 1.70. No information on the second transition is available for the other numerical simulations. Though the present method shows an earlier transition for the first mode change and a delayed transition for the second mode change compared to the experimental data, in the numerical analysis, the jet Mach number at which the non-linear mode transition occurs would be dependent on the numerical techniques adopted for the simulation.

Overall, the present method shows the favorable capability of predicting the amplitude of screech tones except for the jet Mach number between 1.40 and 1.50 where Li & Gao's Navier-Stokes simulation shows the underprediction of the amplitude as well. Since the second mode transition of the present result occurs at the higher jet Mach number than that of the experimental data, the component of C mode is observed even at the jet Mach number 1.80 in the present result. It can be concluded that the present methods can numerically simulate the two three-dimensional modes of screech tones including the non-linear mode transition, and it shows good agreement with the experimental data.

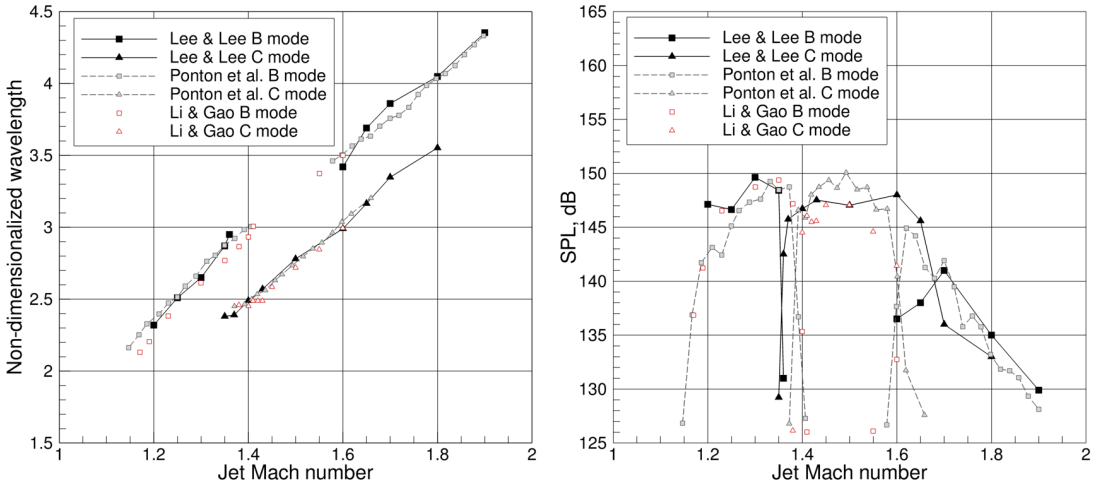

Figure 8 Comparison of the simulated wavelengths and amplitudes of fundamental screech modes with the experimental data and other numerical results

It is interesting to observe that after the second mode transition, from C to B modes, the amplitude of screech tones decreases as the jet Mach number increases. To investigate the tone amplitude qualitatively the spectra of two high jet Mach numbers, 1.70 and 1.90, at various azimuthal angles are plotted in Figure 9. The frequencies of screech tones are marked with dashed lines for reference. When the jet Mach number is 1.7, tones of two modes are clearly observed, which are larger

than the amplitude of other frequencies at all azimuthal angles. When the jet Mach number is 1.9, one tone at the frequency of the B mode is noticeable only at $\varphi = 80$ degrees but its amplitude is smaller than the amplitude of low frequencies. At other azimuthal angles, no screech tone is visible and the spectra looks like a broadband component. It is expected that the screech tone would decrease as the jet Mach number increases further and the jet noise become fully broadband.

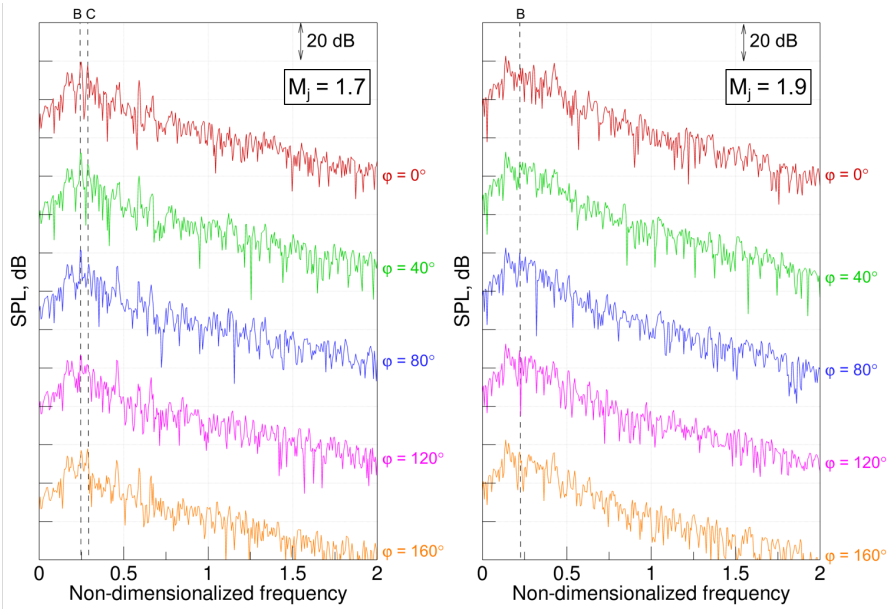

Figure 9 Spectra of two jet Mach numbers at various azimuthal angles (x/D = 0, r/D = 0.889)

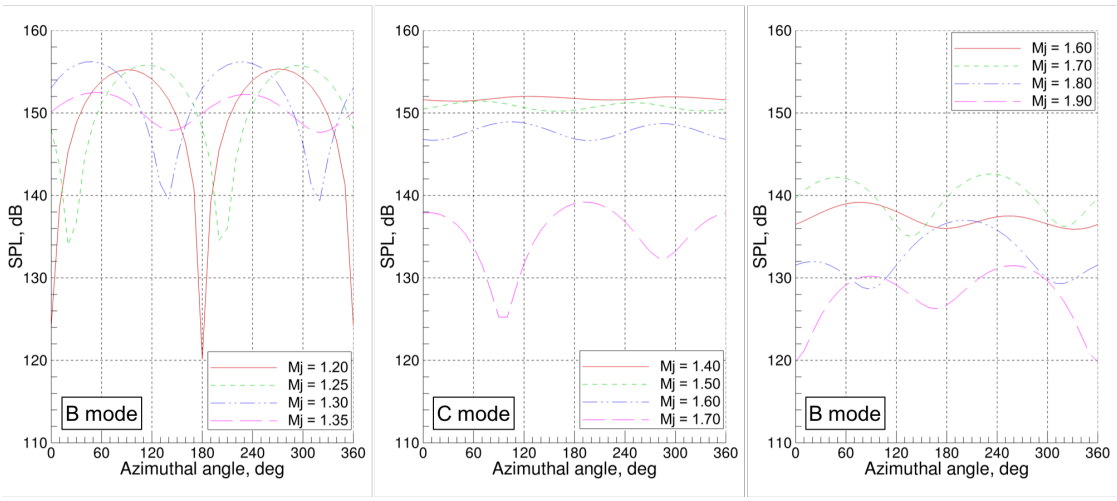

Figure 10 Azimuthal directivity of screech tones at various jet Mach numbers

Figure 10 shows the azimuthal directivity of screech tones at various jet Mach numbers. The left figure shows the azimuthal directivity of the B-mode screech that is observed before the first mode transition. The amplitude variation in the azimuthal direction is more than 35 dB when $M_j = 1.20$, and it reduces down to 5 dB when $M_j = 1.35$. When the first mode change occurs, the C mode is dominant, and it has little azimuthal variation just after the mode transition. When $M_j = 1.60$, the azimuthal variation is 3 dB, and it increases significantly when $M_j = 1.70$ where the B mode becomes dominant after the second mode transition. It is interesting to observe that

the azimuthal directivity of both B and C modes becomes asymmetric after the second mode transition, and the asymmetry in the azimuthal directivity becomes significant as the jet Mach number increases. This can be interpreted as that the flapping motion of a jet stream, which induces a directivity of an acoustic dipole, becomes weaker as the jet Mach number increases, and the screech tone would disappear eventually.

4. CONCLUSIONS

The screech tone of two three-dimensional modes from supersonic underexpanded jet was numerically reproduced using computational aeroacoustics methods. A fourth-order optimized compact scheme and fourth-order Runge-Kutta method were used to solve three dimensional Euler equations. The tool was validated by numerically analyzing the flow structure of two experimental cases: one is the radial Mach number distribution of a perfectly expanded jet of a Mach number of 2.1, and the other is the radial density distribution of three under-expanded jets of a Mach number of 1.43, 1.6, and 1.8. Extensive analysis was performed to investigate the characteristics of two three-dimensional modes B and C modes, of screech tones for various Mach numbers from 1.2 to 1.9. The wavelengths and amplitude of the reproduced screech tones showed good agreement with other results. The present method also predicted two mode transitions: the present method shows an earlier transition for the first mode change and a delayed transition for the second mode change compared to the experimental data. The directivity in the azimuthal direction is also investigated. Before the first mode transition. the azimuthal directivity of a B-mode screech tone resembles that of an acoustic dipole. The amplitude variation in the azimuthal direction is more than 35 dB when $M_j = 1.20$, and it reduces as the jet Mach number increases. The azimuthal directivity is close to that of an acoustic monopole. It is observed that the azimuthal directivity of both B and C modes becomes asymmetric after the second mode transition, and the asymmetry in the azimuthal directivity becomes substantial as the jet Mach number increases. It can be concluded that the present inviscid tool can numerically reproduce the screech tone including its non-linear mode transition without considering a viscous effect.

5. REFERENCES

1. Powell, A., “The Noise of Choked Jets,” *The Journal of the Acoustical Society of America*, vol. 25, May 1953, pp. 385–389.
2. Davis, M. G., and Oldfield, D. E. S., “Tones from a Choked Axisymmetric Jet.I Cell Structure, Eddy Velocity and Source Locations,” *Acustica*, vol. 12, 1962, pp. 257–277.
3. Rosfjord, T. J., and Toms, H. L., “Recent observations including temperature dependence of axisymmetric jet screech,” *AIAA Journal*, vol. 13, Oct. 1975, pp. 1384–1386.
4. Norum, T. D., “Screech suppression in supersonic jets,” *AIAA Journal*, vol. 21, Feb. 1983, pp. 235–240.
5. Seiner, J., Manning, J., and Ponton, M., “Model and full scale study of twin supersonic plume resonance,” 25th AIAA Aerospace Sciences Meeting, 1987.
6. Ponton, M. K., and Seiner, J. M., “The effects of nozzle exit lip thickness on plume resonance,” *Journal of Sound and Vibration*, vol. 154, 1992, pp. 531–549.
7. Panda, J., “An experimental investigation of screech noise generation,” *Journal of Fluid Mechanics*, vol. 378, 1999, pp. 71–96.
8. Edgington-Mitchell, D., Oberleithner, K., Honnery, D. R., and Soria, J., “Coherent structure and sound production in the helical mode of a screeching axisymmetric jet,” *Journal of Fluid Mechanics*, vol. 748, Jun. 2014, pp. 822–847.

9. Mercier, B., Castelain, T., and Bailly, C., “A schlieren and nearfield acoustic based experimental investigation of screech noise sources,” 22nd AIAA/CEAS Aeroacoustics Conference, 2016.
10. Tam, C. K. W., Jackson, J. A., and Seiner, J. M., “A multiple-scales model of the shock-cell structure of imperfectly expanded supersonic jets,” *J. Fluid Mech*, vol. 153, 1985, pp. 123–149.
11. Tam, C. K. W., Seiner, J. M., and Yu, J. C., “Proposed relationship between broadband shock associated noise and screech tones,” *Journal of Sound and Vibration*, vol. 110, Oct. 1986, pp. 309–321.
12. Tam, C. K. W., Parrish, S. A., and Viswanathan, K., “Harmonics of Jet Screech Tones,” *AIAA Journal*, vol. 52, Nov. 2014, pp. 2471–2479.
13. Cain, A., Bower, W., Walker, S., and Lockwood, M., “Modeling supersonic jet screech. I - Vortical instability wave modeling,” 33rd Aerospace Sciences Meeting and Exhibit, 1995.
14. Kandula, M., “A Nonlinear Shock-Refracted Acoustic Wave Model for the Prediction of Screech Amplitude in Underexpanded Supersonic Jets,” 12th AIAA/CEAS Aeroacoustics Conference (27th AIAA Aeroacoustics Conference), 2006.
15. Umeda, Y., and Ishii, R., “Oscillation modes of underexpanded jets issuing from square and equilateral triangular nozzles,” *The Journal of the Acoustical Society of America*, vol. 95, Apr. 1994, pp. 1853–1857.
16. Shen, H., and W. Tam, C. K., “Numerical Simulation of the Generation of Axisymmetric Mode Jet Screech Tones,” *AIAA Journal*, vol. 36, Oct. 1998, pp. 1801–1807.
17. Manning, T., and Lele, S., “Numerical simulations of shock-vortex interactions in supersonic jet screech,” 36th AIAA Aerospace Sciences Meeting and Exhibit, 1998.
18. Outa, E., Shinozawa, Y., Kobayashi, H., Oinuma, H., and Nagai, K., “Computational Study on Supersonic Jet Screech and Suppressing Effect of a Vortex Generator,” Proceedings of the 7th International Congress on Sound and Vibration, 2000.
19. Jorgenson, P., and Loh, C., “Computing Axisymmetric Jet Screech Tones using Unstructured Grids,” 38th AIAA/ASME/SAE/ASEE Joint Propulsion Conference & Exhibit, AIAA-2002-3889, Jul. 2002.
20. Li, X. D., and Gao, J. H., “Numerical simulation of the generation mechanism of axisymmetric supersonic jet screech tones,” *Physics of Fluids*, vol. 17, Aug. 2005, p. 085105.
21. Lee, I. C., and Lee, D. J., “An Analysis of Feedback Process in the Screech Tone from Supersonic Axisymmetric Jet Using an Optimized High Order Compact Scheme,” *Computational Fluid Dynamics Journal*, vol. 16, 2007, pp. 194–202.
22. Shen, H., and Tam, C. K. W., “Three-dimensional numerical simulation of the jet screech phenomenon,” *AIAA Journal*, vol. 40, Jan. 2002, pp. 33–41.
23. Li, X., and Gao, J., “Numerical Simulation of Three-Dimensional Supersonic Jet Screech Tones,” 11th AIAA/CEAS Aeroacoustics Conference, 2005.
24. Li, X., and Gao, J., “Prediction and Understanding of Three-Dimensional Screech Phenomenon from a Circular Nozzle,” 13th AIAA/CEAS Aeroacoustics Conference, 2007.
25. Kurbatskii, K. A., “Numerical Simulation of Three-Dimensional Jet Screech Tones using a General Purpose Finite-Volume CFD code,” 49th AIAA Aerospace Sciences Meeting including the New Horizons Forum and Aerospace Exposition, vol. C, 2011.
26. Gojon, R., and Bogey, C., “Numerical study of the flow and the near acoustic fields of an underexpanded round free jet generating two screech tones,” *International Journal of Aeroacoustics*, vol. 16, 2017, pp. 603–625.

27. Tam, C. K. W., Viswanathan, K., Ahuja, K. K., and Panda, J., "The sources of jet noise: experimental evidence," *Journal of Fluid Mechanics*, vol. 615, Nov. 2008, p. 253.
28. Crow, S. C., and Champagne, F. H., "Orderly structure in jet turbulence," *Journal of Fluid Mechanics*, vol. 48, Aug. 1971, pp. 547–591.
29. Brown, G. L., and Roshko, A., "On density effects and large structure in turbulent mixing layers," *Journal of Fluid Mechanics*, vol. 64, Jul. 1974, pp. 775–816.
30. Loh, C. Y., and Hultgren, L. S., "Jet Screech Noise Computation," *AIAA Journal*, vol. 44, May 2006, pp. 992–998.
31. Viswanathan, K., "Analysis of the Two Similarity Components of Turbulent Mixing Noise," *AIAA Journal*, vol. 40, Sep. 2002, pp. 1735–1744.
32. Mankbadi, R., Hixon, R., Shih, S., and Povinelli, L., "Use of Linearized Euler Equations for Supersonic Jet Noise Prediction," *AIAA Journal*, vol. 36, Feb. 1998, pp. 140–147.
33. Cheng, T. S., and Lee, K. S., "Numerical simulations of underexpanded supersonic jet and free shear layer using WENO schemes," *International Journal of Heat and Fluid Flow*, vol. 26, Oct. 2005, pp. 755–770.
34. Lee, I., and Lee, D. J., "Investigation on the Source Locations of Axisymmetric Screech Tones Utilizing Data from Numerical Simulation," *Journal of Theoretical and Computational Acoustics*, Oct. 2018, p. 1850058.
35. Lele, S. K., "Compact finite difference schemes with spectral-like resolution," *Journal of Computational Physics*, vol. 103, Nov. 1992, pp. 16–42.
36. Tam, C. K. W., and Webb, J. C., "Dispersion-Relation-Preserving Finite Difference Schemes for Computational Acoustics," *Journal of Computational Physics*, vol. 107, Aug. 1993, pp. 262–281.
37. Kim, J. W., and Lee, D. J., "Optimized compact finite difference schemes with maximum resolution," *AIAA Journal*, vol. 34, May 1996, pp. 887–893.
38. Kim, J. W., and Lee, D. J., "Generalized Characteristic Boundary Conditions for Computational Aeroacoustics," *AIAA Journal*, vol. 38, Nov. 2000, pp. 2040–2049.
39. Kim, J. W., and Lee, D. J., "Adaptive Nonlinear Artificial Dissipation Model for Computational Aeroacoustics," *AIAA Journal*, vol. 39, May 2001, pp. 810–818.
40. Lee, I. C., and Lee, D. J., "An analysis of flow and screech tone from supersonic axisymmetric jet at the initial stage," *Journal of Mechanical Science and Technology*, vol. 22, Apr. 2008, pp. 819–826.
41. Ponton, M. K., Seiner, J. M., and Brown, M. C., "Near Field Pressure Fluctuations in the Exit Plane of a Choked Axisymmetric Nozzle," NASA Technical Memorandum 113137, 1997.
42. Trouttt A N, T. R., and Mclaughlins, D. D. K., "Experiments on the flow and acoustic properties of a moderate-Reynolds-number supersonic jet," *J. Fluid Mech*, vol. 116, 2017, pp. 123–156.
43. Kim, Y.-S., "Analysis of radiated noise from internal duct flow and external jet using high-resolution schemes," Ph. D. Dissertation, Korea Advanced Institute of Science and Technology, 2001.
44. Panda, J., and Seasholtz, R. G., "Measurement of shock structure and shock-vortex interaction in underexpanded jets using Rayleigh scattering," *Physics of Fluids*, vol. 11, 1999, pp. 3761–3777.